THE JOURNAL OF BIOLOGICAL CHEMISTRY VOL. 290, NO. 8, pp. 5105–5116, February 20, 2015

Subunit-specific Regulation of *N*-Methyl-D-aspartate (NMDA) Receptor Trafficking by SAP102 Protein Splice Variants*

Received for publication, July 25, 2014, and in revised form, December 26, 2014 Published, JBC Papers in Press, January 2, 2015, DOI 10.1074/jbc.M114.599969

Zhe Wei, Blake Behrman, Wei-Hua Wu, and Bo-Shiun Chen[1]

From the Department of Neuroscience and Regenerative Medicine and Department of Neurology, Medical College of Georgia, Georgia Regents University, Augusta, Georgia 30912

Background: SAP102 is a scaffolding protein that regulates NMDA receptor function.
Results: Specific SAP102 spliced isoform is enriched at synapses to regulate NMDA receptor surface expression.
Conclusion: I2 region-containing SAP102 is required for the regulation of subunit-specific NMDA receptor surface expression.
Significance: This is the first study showing that SAP102 synaptic targeting is critical for regulating NMDA receptor trafficking.

Synapse-associated protein 102 (SAP102) is a scaffolding protein abundantly expressed early in development that mediates glutamate receptor trafficking during synaptogenesis. Mutations in human SAP102 have been reported to cause intellectual disability, which is consistent with its important role during early postnatal development. SAP102 contains PDZ, SH3, and guanylate kinase (GK)-like domains, which mediate specific protein-protein interactions. SAP102 binds directly to *N*-methyl-D-aspartate receptors (NMDARs), anchors receptors at synapses, and facilitates transduction of NMDAR signals. Proper localization of SAP102 at the postsynaptic density is essential to these functions. However, how SAP102 is targeted to synapses is unclear. In the current study we find that synaptic localization of SAP102 is regulated by alternative splicing. The SAP102 splice variant that possesses a C-terminal insert (I2) between the SH3 and GK domains is highly enriched at dendritic spines. We also show that there is an intramolecular interaction between the SH3 and GK domains in SAP102 but that the I2 splicing does not influence SH3-GK interaction. Previously, we have shown that SAP102 expression promotes spine lengthening. We now find that the spine lengthening effect is independent of the C-terminal alternative splicing of SAP102. In addition, expression of I2-containing SAP102 isoforms is regulated developmentally. Knockdown of endogenous I2-containing SAP102 isoforms differentially affect NMDAR surface expression in a subunit-specific manner. These data shed new light on the role of SAP102 in the regulation of NMDAR trafficking.

PSD-95-like membrane-associated guanylate kinases (PSD-MAGUKs),[2] including PSD-95, SAP102, PSD-93, and SAP97, are a family of scaffolding proteins highly enriched in the PSD and play essential roles in synaptic organization and plasticity (1). They interact directly or indirectly with major types of glutamate receptors. PSD-MAGUKs possess three PDZ domains, a SH3 domain, and a guanylate kinase (GK) domain. Whereas the PDZ domains bind to cell adhesion molecules, ion channels, and receptors, the SH3 and GK domains interact with cytoskeletal proteins and intracellular signaling complexes. Unlike other members of the family that contain palmitoylated cysteines that are important for synaptic targeting, SAP102 is not palmitoylated on its multiple cysteines (2).

Although genetic studies have shown that PSD-MAGUKs can functionally compensate for each other (3), each PSD-MAGUK member has unique properties and distinct expression patterns (4). For instance, the expression of SAP102 begins early and it is implicated in trafficking and anchoring NMDARs during synaptogenesis (5, 6), whereas PSD-95 is expressed later and is involved in maturation and stabilization of excitatory synapses (7). Consistently, studies have shown that knockdown of SAP102 during early development reduces NMDAR-mediated excitatory postsynaptic current, whereas PSD-95 knockdown has no effect, indicating that SAP102 is crucial for synaptic trafficking of NMDARs during synaptogenesis (8).

NMDARs are voltage-dependent, ligand-gated ion channels that are pivotal in controlling synaptic plasticity and memory function (9). Functional NMDARs are tetramers composed of two essential GluN1 subunits and two regulatory GluN2 (GluN2A-GluN2D) subunits (10). NMDARs formed by different GluN1-GluN2 subunit combinations exhibit distinct channel properties imparted by the GluN2 subunits. During development, the subunit composition of synaptic NMDARs changes from mainly GluN2B- to GluN2A-containing receptors. The GluN2 subunit switch plays a key role in modulating the threshold for inducing synaptic plasticity at different developmental stages (11, 12). Interestingly, the expression patterns of PSD-95 and SAP102 during development are similar to those of GluN2A and GluN2B, respectively (4). As such, PSD-95 and SAP102 has been proposed to differentially regulate NMDAR trafficking in a subunit-specific manner (13). PSD-95 has been shown to regulate the GluN2 subunit switch. Whether SAP102 is involved in this process is not clear.

SAP102 has three naturally occurring splice isoforms that result from two alternatively spliced regions named I1 and I2 (Fig. 1*A*) (14). The I1 region is located in the N terminus of

* This work was supported, in whole or in part, by National Institutes of Health Career Transition Awards R00NS057266 (NINDS; to B.-S. C.) and 1K22CA122453 (NCI; W.-H. W.).
[1] To whom correspondence should be addressed: Dept. of Neuroscience and Regenerative Medicine and Dept. of Neurology, Medical College of Georgia, Georgia Regents University, CA3008, 1120 15th Street, Augusta, GA 30912. Tel.: 706-721-5926; Fax: 706-721-8752; E-mail: bochen@gru.edu.
[2] The abbreviations used are: PSD-MAGUK, PSD-95-like membrane-associated guanylate kinases; GK guanylate kinase; NMDAR, NMDA receptor; aa, amino acid; DIV, days *in vitro*; p-, postnatal.

SAP102, whereas the I2 region is located within a hinge region between the SH3 and GK domains. In previous studies we characterized the I1 region of SAP102 and revealed its function in NMDAR trafficking and spine morphology (15, 16). Here we investigated the role of the I2 region of SAP102. We found that deletion of the I2 region reduces SAP102 enrichment in dendritic spines. We also showed that the SH3 domain of SAP102 interacts with the GK domain, and I2 deletion does not affect this intramolecular interaction. In addition, the spine lengthening effect induced by I1 region-containing SAP102 isoform is independent of the I2 region. Furthermore, RNAi knockdown of I2 region-containing SAP102 differentially affects surface expression of GluN2A and GluN2B. Thus, our findings provide evidence that spine enrichment of SAP102 is involved in the regulation of subunit-specific NMDAR trafficking.

EXPERIMENTAL PROCEDURES

DNA Constructs—FLAG-SAP102ΔI2 was constructed by deleting the DNA fragment between amino acids (aa) 625 and 638 using site-directed mutagenesis. SAP102ΔSH3GK was generated by mutating Tyr-483 to a stop codon (TAT to TAG). The following domains were generated by PCR and subcloned into the LexA DNA binding domain fusion vector pBHA or the Gal4 activation domain fusion vector pGAD10/pGADT7 for yeast two-hybrid binding assays. pBHA constructs: SAP102 SH3, aa 519–591; SAP102 SH3-GK, aa 519–849; SAP102 SH3-GKΔI2 aa 519–624 + 639–849; GKAP95, aa 1–692; GKAP130, aa 1–992. pGAD10 constructs: SAP102 SH3, aa 519–591; SAP102 GK, aa 595–849; SAP102 SH3-GK, aa 519–849; SAP102 SH3-GKΔI2, aa 519–624 + 639–849; mPins, aa 366–483. pGADT7 constructs: SPAR C terminus (GAP-PDZ-Act2-GKBD), aa 585–1822. Short hairpin RNA (shRNA) oligonucleotides were inserted into vector FHUGW. The following shRNA targeting sequence was used for rat I2 region-containing SAP102, AAGGGAGTGACATCCAACA (nucleotide 2215–2233). shRNA-proofed Myc-SAP102 was made by changing G to C at nucleotide 2223 using site-directed mutagenesis.

Antibodies—Rabbit antibodies recognizing SAP102(I2) were generated by Pocono Rabbit Farm and Laboratory. Rabbits were immunized with a synthetic peptide Ac-GVTSNTSDSES-SSC-OH corresponding to amino acids 626–638 of SAP102. Sera were collected and affinity-purified using the antigen peptide. The SAP102(I2) antibodies were not suitable for immunocytochemistry. Monoclonal anti-FLAG was purchased from Sigma. Pan-SAP102 antibody was purchased from NeuroMab (Antibodies, Inc.).

Subcellular Fractionation—Synaptic and extrasynaptic membranes were enriched as described previously with minor modifications (24). Briefly, P4 rat forebrain was homogenized in sucrose buffer (320 mM sucrose, 20 mM HEPES pH 7.4, 5 mM EDTA, and Pierce Protease Inhibitor) and centrifuged at 1000 × *g* for 7 min. The resulting supernatant was centrifuged at 10,000 × *g* for 20 min. The pellet was lysed by hypo-osmotic shock in water, during which HEPES was added rapidly to a final concentration of 1 mM. This lysate was subjected to detergent extraction in the presence of 0.5% Triton X-100. The suspension was mixed constantly at 4 °C for 20 min followed by centrifugation at 32,000 × *g* for 20 min. The supernatant (TxS) contained proteins loosely attached to the PSD (biochemically defined as extrasynaptic membrane fraction), and the pellet (TxP) contained proteins tightly bound to the PSD (biochemically defined as synaptic membrane fraction). The TxP fraction was then solubilized with 1% SDS. For every centrifugation step above, pellets were rinsed twice with sucrose buffer to avoid potential contamination between fractions. Concentration of TxP and TxS was measured, and equal amounts of proteins were loaded for Western blot analysis.

Immunoblots—Whole rat brain lysate was collected at various ages. The crude synaptosome (P2) fraction was prepared as described previously (17). The P2 lysate was resolved by 10% SDS-PAGE and analyzed by Western blot with either pan-SAP102 antibody (detects all SAP102 splice variants) or with I2-specific SAP102 antibody. The experiment was repeated three times and quantified using ImageQuant software. All ages were normalized to the intensity at P2, and then a ratio of SAP102(I2) to total SAP102 was determined. The average ratio is shown.

Neuronal Cultures and Immunocytochemistry—Primary hippocampal cultures were prepared from embryonic day 19 (E19) Sprague-Dawley rats. Dissociated neurons were plated on poly-D- lysine-coated coverslips in Neurobasal medium supplemented with B27 and L-glutamine. Hippocampal neurons were transfected at 12 days *in vitro* (DIV) using Lipofectamine (Lipofectamine LTX and Plus Reagent; Invitrogen). Neurons were fixed at DIV14 in 4% paraformaldehyde for 15 min, permeabilized with 0.25% Triton X-100, PBS and blocked in 10% normal goat serum, PBS. Cells were incubated with primary antibodies against FLAG in PBS, 3% normal goat serum, washed, and incubated with secondary antibodies (Alexa 488) in PBS, 3% normal goat serum against mouse IgG1. The cells were mounted onto coverslips (Prolong Antifade kit; Invitrogen). For surface expression analysis, transfected neurons were incubated with anti-FLAG antibody (Sigma) for 30 min at room temperature to label surface-expressed protein. The cells were fixed in 4% paraformaldehyde for 15 min and incubated with Alexa 647-conjugated (green) anti-mouse secondary antibody (molecular Probes) for 30 min. The cells were permeabilized with 0.25% Triton X-100, incubated with 10% normal goat serum, and labeled with anti-FLAG antibody (Sigma) for 30 min at room temperature. After extensive washing, cells were incubated with Alexa 568-conjugated (red) anti-mouse secondary antibody for 30 min and mounted with a Prolong Antifade kit. Images were collected with a 63× objective on a Zeiss LSM 700 confocal microscope. A series of optical sections collected at intervals of 0.5 μm was used to create maximum projection images. For quantitative analysis, images from three dendrites per neuron were collected, and the fluorescence intensity was quantitated using ImageJ software. At least three independent experiments were performed per condition. The number of experiments (*N*) and neurons (*n*) for each condition is indicated in the corresponding figure legends. *n* is used in statistical analysis.

Transfection—HEK-293 cells were seeded at 20–25% confluency the day before transfection. Cells were transiently transfected with plasmids using the calcium phosphate method as

described previously (18). Cells were harvested 24 h after transfection for Western blot analysis.

Lentivirus Production and Neuronal Infection—For lentiviral particle production, HEK-293T cells were co-transfected with FHUGW constructs (dual-promoter pUbiquitin-EGFP/pH1-shRNA) and helper vectors pDelta8.9 and pVSVg using Lipofectamine LTX (Invitrogen). Two days after transfection, supernatant was collected and concentrated by ultrafiltration in Centricon Plus 100 (Millipore). Virus particles were aliquoted and stored at −80 °C. Particle titer was determined by infection of HEK-293T cells. Cultured hippocampal neurons were infected with appropriate amounts of virus particles at DIV4, which resulted in ~80–90% of infection efficiency. Neurons were then harvested at DIV14 for Western blot analysis.

Image Acquisition and Analysis—Images were collected with a 63× objective on a Zeiss LSM 700 confocal microscope. A series of optical sections collected at intervals of 0.5 μm was used to create maximum projection images. Neurons were selected randomly from each coverslip with the viewer blinded to the experimental conditions. At least three independent experiments were performed per condition, and the number of neurons for each condition is indicated in the corresponding figure legend. The immunochemistry data were analyzed using ImageJ software (NIH). Spine/dendrite ratio was analyzed as described previously (19). Mushroom spines of secondary dendrites and adjacent dendrite shaft regions were defined under the DsRed channel. Then, under the FLAG channel, the regions of interest were reloaded. The mean intensity of FLAG-tagged protein in spine regions and dendrite regions was measured. Dendritic spines were measured as described previously (16). Spine length was measured by manually drawing a line from the base of the spine neck to the furthest point at the end of the spine. The cumulative frequency plots were constructed by sorting the length or width in bins of 0.5- or 0.3-μm size and using a discrete variable on the horizontal axis. The ordinal axis was labeled with percentages. Measurements were analyzed in Microsoft Excel, and statistical significance was determined by Student's *t* test.

Biotinylation Assay—Cultured cortical neurons (DIV14–16) were washed 3 times with progressively cooler PBS containing 1 mM $MgCl_2$, 2.5 mM $CaCl_2$ (PBS+) and incubated with 1 mg/ml EZ-Link Sulfo-NHS-LC-biotin (Pierce) in PBS+ for 20 min at 4 °C with gentle agitation. Cells were washed 3 times with ice-cold quenching buffer (50 mM glycine in PBS+) for 5 min each. The cells were then scraped into cold lysis buffer (50 mM Tris, pH 7.4, 2 mM EDTA, 2 mM EGTA, and proteinase inhibitor) and sonicated. Lysate was centrifuged at 100,000 × *g* for 20 min at 4 °C to obtain a crude membrane fraction. The crude membrane fraction was first lysed in 1% SDS for 30 min at 37 °C and then in 1% Triton X-100 at 4 °C, both in lysis buffer with 100 mM NaCl. The lysate was centrifuged at 100,000 × *g* for 20 min and then incubated with streptavidin-Sepharose beads (Pierce) for 2 h at 4 °C with gentle rotation. Beads were washed 4 times in washing buffer containing 1% Triton X-100. Biotinylated membrane proteins were eluted in SDS-PAGE sample buffer.

Yeast Two-hybrid Assay—The yeast two-hybrid assay was performed as described previously (18). Briefly, pBHA and pGAD10/pGADT7 constructs were co-transformed into the L40 yeast strain. After transformation, cells were plated in synthetic complete medium lacking leucine and tryptophan. Three independent yeast colonies were selected and assayed for expression of the reporter HIS3 gene in synthetic complete medium lacking leucine, tryptophan, and histidine.

RNA Extraction and Quantitative Real-time PCR Analysis—Rat forebrain was homogenized in TRIzol reagent (Invitrogen), and RNA was isolated according to the manufacturer's protocol. cDNA synthesis of RNA was performed using the Maxima First Strand cDNA Synthesis kit (Thermo scientific). Quantitative real-time PCR was performed using SsoAdvanced Universal SYBR Green Supermix (Bio-Rad) with CFX96 Touch™ Real-Time PCR Detection System (Bio-Rad). Primer sequences are as follows: I2-containing SAP102, forward (5′-CGGGACTTCCCTGGGTTA-3′), reverse (5′-GGAACTGCTTTCGCTGTCA-3′); pan-SAP102, forward (5′-AGAGACTGCAGCAAGCACAA-3′), reverse (5′-CCAGTTTCATGGCTTTGTCA-3′). A standard curve for each gene was generated by serial dilutions of a standard. The PCR amplification efficiency is 104% for I2-contaning SAP102 primers and 99% for pan-SAP102 primers. The experiments were repeated three times, and quantification was performed using the ΔCT method.

RESULTS

PSD-MAGUKs play important roles in basal synaptic transmission as well as activity-dependent synaptic plasticity (20). All of these functions rely on proper localization of PSD-MAGUKs at the PSD. Posttranslational modifications including palmitoylation, ubiquitination, and phosphorylation are critical for controlling synaptic localization of PSD-95 (21–23). However, how SAP102 is targeted to synapses remains unclear. Previous studies have shown that SAP102 stabilization at postsynaptic sites is dependent on the SH3 and GK domains (19). Interestingly, the I2 region of SAP102 is located within the hinge region between the SH3 and GK domains (Fig. 1*A*). To investigate whether the synaptic localization of SAP102 is regulated by I2 alternative splicing, we made a SAP102 construct lacking the I2 region (SAP102ΔI2) to mimic I2 splicing. A SAP102 construct lacking the SH3 and GK domains (SAP102ΔSH3GK) was used as a control. The spine enrichment was quantified by determining spine/dendrite fluorescence ratios in primary hippocampal neurons expressing FLAG-tagged SAP102, SAP102ΔI2, or SAP102ΔSH3GK. We coexpressed DsRed to define spine and adjacent dendrite shaft region and stained with anti-FLAG to visualize distributions of SAP102 in neurons. Consistent with previous results, SAP102ΔSH3GK was present throughout the cell indistinguishable from DsRed alone (Fig. 1*B*). Interestingly, neurons expressing SAP102ΔI2 displayed reduced synaptic targeting compared with SAP102 (Fig. 1*B*). The spine/dendrite green fluorescence ratio of SAP102ΔI2 was 1.9 ± 0.05, an ~1.6-fold decrease compared with the ratio of SAP102 (3 ± 0.09, $p < 0.05$), and an ~1.9-fold increase compared with the ratio of SAP102ΔSH3GK (0.98 ± 0.03, $p < 0.05$) (Fig. 1*C*). To determine whether the endogenous I2-region containing SAP102 is enriched at synapses, we raised an antibody that specifically recognizes I2 region-containing SAP102 (SAP102(I2)) and does not cross-react with the other members of PSD-MAGUKs (Fig.

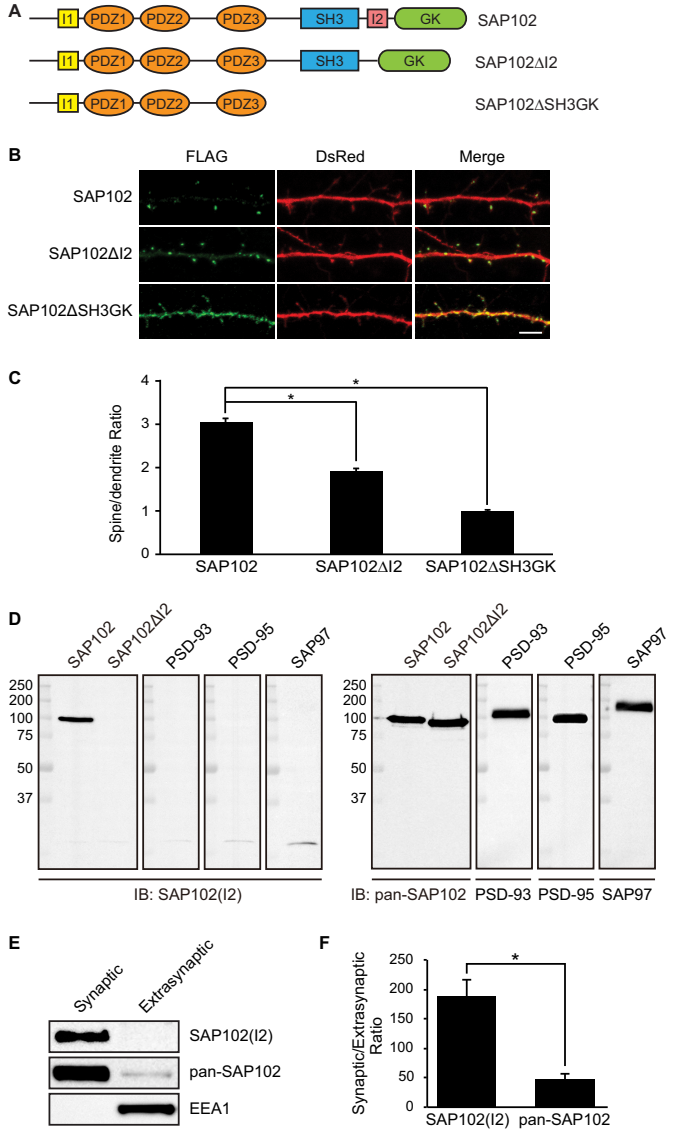

FIGURE 1. **The I2 region is important for SAP102 clustering in spines.** *A*, schematic domain structures of two naturally occurring splice variants of SAP102 (SAP102 and SAP102 ΔI2) and a C-terminal truncated form used in this study. SAP102 contains both I1 and I2 regions. SAP102ΔI2 contains a 14-aa deletion of the I2 region between the SH3 and GK domains (14). *B*, hippocampal neurons were co-transfected with FLAG-SAP102/DsRed, FLAG-SAP102ΔI2/DsRed, or FLAG-SAP102ΔSH3GK/DsRed. SAP102ΔI2 displayed reduced synaptic targeting. FLAG-SAP102 is enriched in spines. FLAG-SAP102ΔSH3GK is uniformly distributed throughout the dendrite and the spines. *Scale bar*, 5 μm. *C*, the mean fluorescence intensity of spines compared with that in adjacent dendrites. The spine/dendrite green fluorescence ratio of FLAG-SAP102, FLAG-SAP102ΔI2, and FLAG-SAP102ΔSH3GK is 3 ± 0.09, 1.9 ± 0.05, and 0.98 ± 0.03, respectively. $n = 10–15$ neurons from three transfections. *, $p < 0.05$, *t* test with Bonferroni's correction after ANOVA. *D*, HEK-293 cells were transfected with SAP102, SAP102ΔI2, PSD-93, PSD-95, or SAP97, and immunoblots (*IB*) of cell lysate were probed with pan-SAP102, SAP102 I2-specific, PSD-93, PSD-95, or SAP97 antibody. *E*, distribution of proteins in synaptic and extrasynaptic membrane fractions. Equal amounts of total proteins were loaded from each of the fractions and probed with I2-specific SAP102 antibody, pan-SAP102 antibody (detects all SAP102 splice variants), and the early endosomal marker EEA1 antibody. *F*, ratio of synaptic to extrasynaptic membrane fractions of SAP102(I2) and total SAP102. Data represent the means ± S.E. The experiment was repeated three times and quantified using ImageQuant LAS TL software. *, $p < 0.05$, Student's *t* test.

1*D*). Using a previously described detergent extraction approach, synaptic and extrasynaptic membrane fractions were enriched based on Triton X-100 solubility (24). We found that both I2 region-containing SAP102 and total SAP102 were highly enriched in synaptic fraction (Fig. 1*E*). Quantitative analysis showed that the ratio of synaptic to extrasynaptic fraction of SAP102(I2) is markedly greater than that of total SAP102 (Fig. 1*F*), suggesting that almost all, if not all, I2 region-containing SAP102 is localized at synapses. EEA1, a marker for early endosome, was only detected in the extrasynaptic membrane fractions, confirming no cross-contamination between the two fractions. These data indicate that the I2 region contributes to SAP102 clustering in dendritic spines, suggesting a specific role of I2-containing SAP102 splice variants in regulating synaptic function.

How does the I2 region facilitate synaptic targeting of SAP102? Previous studies have shown that there is an inter- or intramolecular interaction between the SH3 and GK domains (25–27). The intramolecular association, dependent on the hinge region between the SH3 and GK domains, dominates and precludes intermolecular interaction. Interestingly, it has been reported that this intramolecular interaction in SAP97 plays an essential role in its synaptic recruitment and assembly (27). The intramolecular interaction between the SH3 and GK domains of PSD-95, SAP97, or PSD-93 has been demonstrated by several groups; however, whether the SH3 and GK domains in SAP102 can bind to each other has not been tested. Therefore, we investigated whether the SH3 domain of SAP102 binds to the GK domain using a yeast two-hybrid binding assay, a system that has been used to examine intramolecular interactions between the SH3 and GK domains. We observed a His+ phenotype in yeast co-transformed with the DNA binding domain fusion construct carrying the SAP102 SH3 domain and the activation-domain fusion construct containing the GK domain, demonstrating that the SH3 domain can bind to the GK domain (Fig. 2*A*). Furthermore, we found that the interaction between the SH3 and GK domains occurred predominantly in an intramolecular mode because the SH3-GK construct did not bind to the SH3 domain (Fig. 2*A*). This is consistent with the previous characterization of the intramolecular interactions between the SH3 and GK domains in the other members of PSD-MAGUK family. We next investigated if the I2 region plays a role in the intramolecular interaction by examining the interaction between SH3 and SH3-GK ΔI2. We observed no effect of I2 deletion on intramolecular interaction (Fig. 2*A*). A number of binding partners of the PSD-MAGUK SH3/GK domain have been identified, including spine-associated Rap-specific GTPase-activating protein (SPAR), guanylate kinase-associated protein (GKAP), and mammalian homologue of *Drosophila melanogaster* partner of inscuteable (mPins) (28–30). In an effort to identify SAP102 interacting proteins that can be regulated by the I2 region, we examined the interactions of SAP102 SH3-GK (+/−) with these previously identified proteins using the yeast two-hybrid binding assay. We found that although the full-length SAP102 SH3-GK binds these proteins, deletion of I2 does not affect any of the interactions (Fig. 2, *B–D*).

In previous studies we have shown that SAP102 splice variants differentially affect spine morphology (16). Neurons expressing SAP102 (contains both I1 and I2) have longer dendritic spines, whereas the spine length of SAP102ΔI1 expressing neurons is similar to DsRed alone. To investigate whether

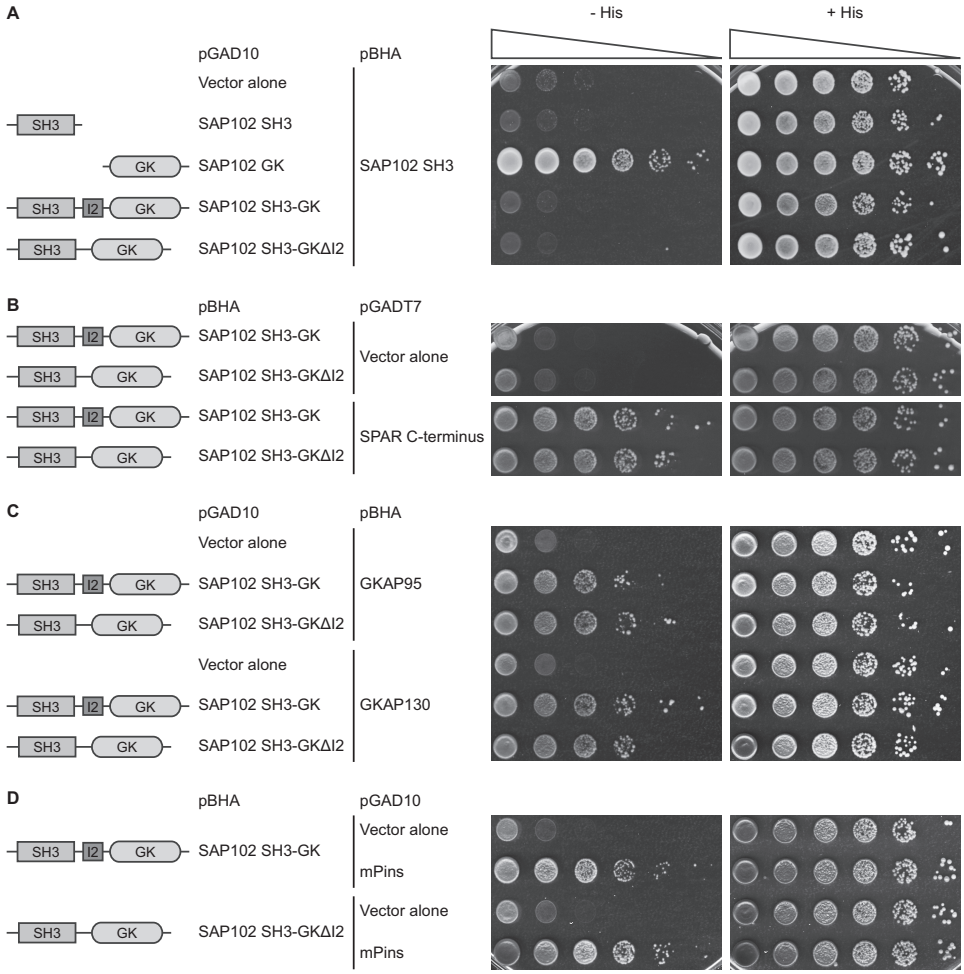

FIGURE 2. **Deletion of the I2 region does not affect the intramolecular interaction between the SH3 and GK domains in SAP102 and the SPAR, GKAP, and mPins binding.** Yeast were co-transformed with pBHA-SAP102 SH3 and pGAD10-SAP102 SH3, GK, SH3-GK or SH3-GKΔI2 (*A*), pGADT7-SPAR C terminus and pBHA-SAP102 SH3-GK or SH-GKΔI2 (*B*), pGAD10-SAP102 SH3-GK or SH-GKΔI2 and pBHA-GKAP95 or GKAP130 (*C*), and pGAD10-SAP102 SH3-GK or SH-GKΔI2 and pBHA-mPins (*D*), and growth was evaluated on appropriate yeast selection medium. Results shown are 10-fold serial dilutions of yeast cells.

the I2 region is required for the spine lengthening effect of SAP102, we next examined spine morphology in primary hippocampal neurons (DIV14) expressing FLAG-tagged SAP102, SAP102ΔI2, or SAP102ΔSH3GK. Neurons were stained with anti-FLAG to assess SAP102 expression levels, and DsRed was co-expressed to visualize the morphology of transfected neurons. Consistent with our previous findings, neurons expressing FLAG-SAP102 had significantly longer dendritic spines (Fig. 3*A*). Similar to FLAG-SAP102, spine length of FLAG-SAP102ΔI2 and FLAG-SAP102ΔSH3GK expressing neurons was significantly longer than that of DsRed alone (Fig. 3*A*). The mean length of dendritic spines was increased in neurons expressing FLAG-SAP102 (from 1.55 ± 0.03 to 2.09 ± 0.06), FLAG-SAP102ΔI2 (from 1.55 ± 0.03 to 2.10 ± 0.06), or FLAG-SAP102ΔSH3GK (from 1.55 ± 0.03 to 2.20 ± 0.07) (Fig. 3*B*). Spine width did not differ among SAP102/DsRed-, SAP102ΔI2/DsRed-, and DsRed-expressing neurons (Fig. 3*A*). Interestingly, expression of FLAG-SAP102ΔSH3GK causes a significant increase of spine width (from 0.50 ± 0.01 to 0.60 ± 0.01) (Fig. 3*B*). Cumulative frequency plots of spine length revealed that overexpression of SAP102, SAP102ΔI2, or SAP102ΔSH3GK resulted in a rightward shift in spine length, indicating that both SAP102 splice variants and the SH3-GK domain truncated mutant substantially increased the proportion of long spines (Fig. 3*B*). Unlike SAP102ΔSH3GK, no significant difference in the cumulative frequency of spine width was observed in SAP102 or SAP102ΔI2 (Fig. 3*B*). In addition, the spine density was not changed significantly in neurons expressing SAP102, SAP102ΔI2, or SAP102ΔSH3GK (Data not shown). Thus, our findings indicate that the I2 region is not required for the spine lengthening effect of SAP102.

SAP102 splice variants containing the I1 region (SAP102 and SAP102ΔI2) have unique expression patterns during development (16). The peak expression of the I1 region-containing SAP102 (SAP102(I1)) occurs between postnatal day 7 (P7) and P11, which coincides with a time critical for the development of dendritic filopodia. To determine whether expression of the SAP102 splice variants containing the I2 region (SAP102 and SAP102ΔI1) is developmentally regulated, Western blot analysis was performed using homogenized rat brain lysate measuring total levels of SAP102 and SAP102(I2). Both SAP102(I2) and total SAP102 levels increase during the first three postnatal weeks (Fig. 4*A*). Quantification of the Western blots showed that the ratio of SAP102(I2) to total SAP102 levels decreases

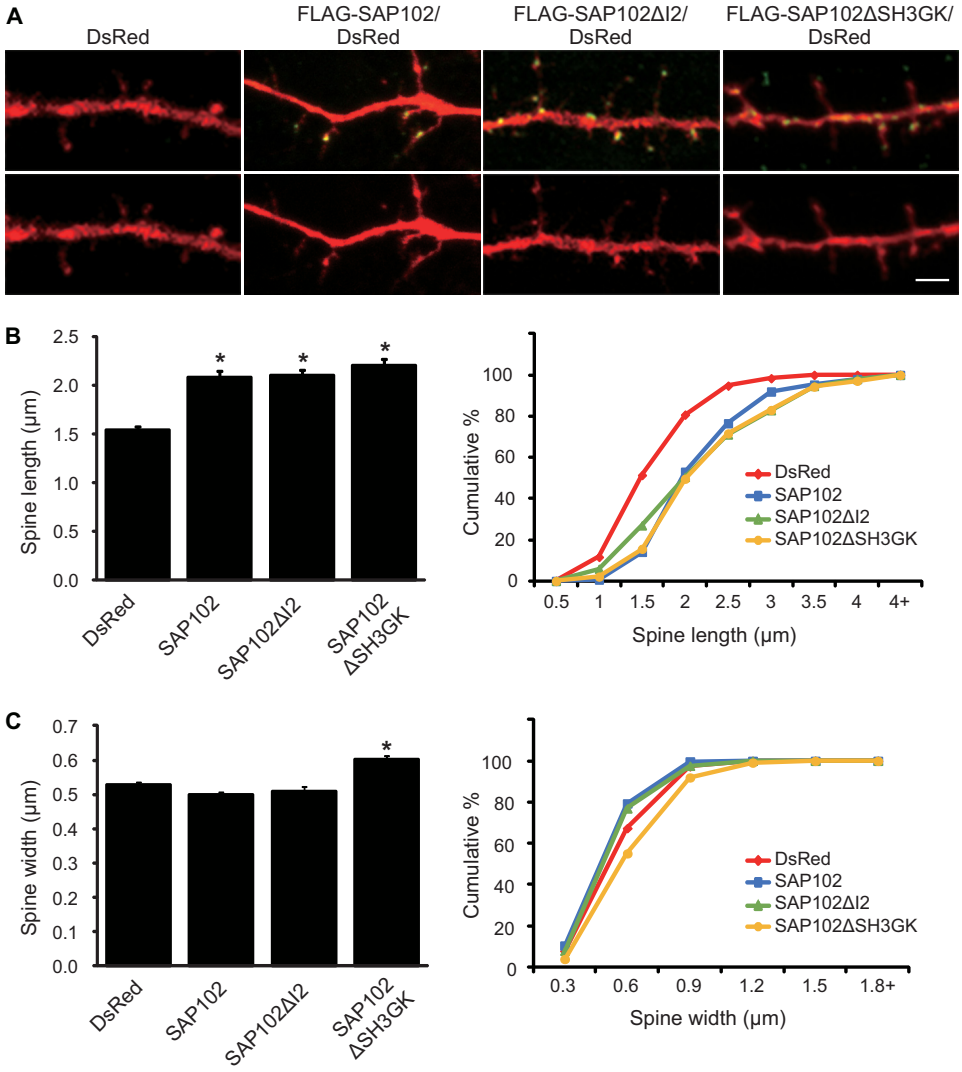

FIGURE 3. **SAP102 splice variants regulate spine morphology.** *A*, primary hippocampal neurons (DIV12) were transfected with FLAG-SAP102/DsRed, FLAG-SAP102ΔI2/DsRed, FLAG-SAP102ΔSH3GK, or DsRed only. At DIV14, they were fixed and labeled with anti-FLAG antibody (*green*). *Scale bar*, 2 μm. *B*, dendritic spines were quantified by measuring DsRed signal using ImageJ software. Dendrites on neurons transfected with FLAG-SAP102/DsRed or FLAG-SAP102ΔI2/DsRed had longer protrusions than those transfected with FLAG-SAP102 ΔSH3GK/DsRed or DsRed only. *C*, cumulative frequency plots of spine length and spine width are shown. Data represent the means ± S.E. ($n = 10$ neurons per condition from 3 independent cultures; 20–30 spines/neuron; *, $p < 0.05$, *t* test with Bonferroni's correction after ANOVA).

significantly during P2 to P8 (Fig. 4*A*), suggesting that SAP102(I2) plays an important role in early period of postnatal development. We next analyzed the ratio of SAP102(I2) to total SAP102 expression using quantitative real-time PCR at P2 and P20. At P2, expression of SAP102(I2) accounts for ~35% of total SAP102 (Fig. 4*B*). Consistent with the protein expression ratios in Fig. 4*B*, the relative expression of SAP102(I2) decreased to ~25% of total SAP102 at P20.

SAP102 mediates synaptic NMDAR trafficking. However, whether synaptic enrichment of SAP102 is involved in the regulation process is unknown. To investigate whether endogenous I2-containing SAP102 plays a role in regulating NMDAR surface expression, we generated shRNA to specifically knock down expression of I2 region-containing SAP102. We tested the specificity of the shRNA by co-expression with SAP102, SAP102ΔI2, PSD-95, PSD-93, or SAP97 in HEK-293 cells. SAP102 I2 shRNA selectively knocked down expression of SAP102 and had no effect on SAP102ΔI2, PSD-95, PSD-93, and SAP97 expression (Fig. 5*A* and data not shown). We next examined the effect of SAP102 I2 shRNA on the expression of I2 region-containing SAP102 in primary hippocampal neurons infected with lentivirus expressing SAP102 I2 shRNA. SAP102 I2 shRNA efficiently reduced expression of I2 region-containing SAP102 and lentivirus expressing a control scrambled shRNA had no effect (Fig. 5*B*). In addition, knockdown of I2 region-containing SAP102 did not affect expression of the other PSD-MAGUKs (data no shown).

To examine the effect of SAP102 I2 shRNA, we infected cultured hippocampal neurons with lentivirus at DIV4 and overexpressed FLAG-GluN2A or FLAG-GluN2B at DIV14 to examine NMDAR surface expression. Neurons expressing SAP102 I2 shRNA had significantly increased surface FLAG-GluN2A and reduced surface FLAG-GluN2B compared with control shRNA expressing neurons (Fig. 6, *A* and *B*). Furthermore, coexpression of a shRNA-proofed I2 region-containing SAP102 rescued the observed effect of SAP102 I2 shRNA on

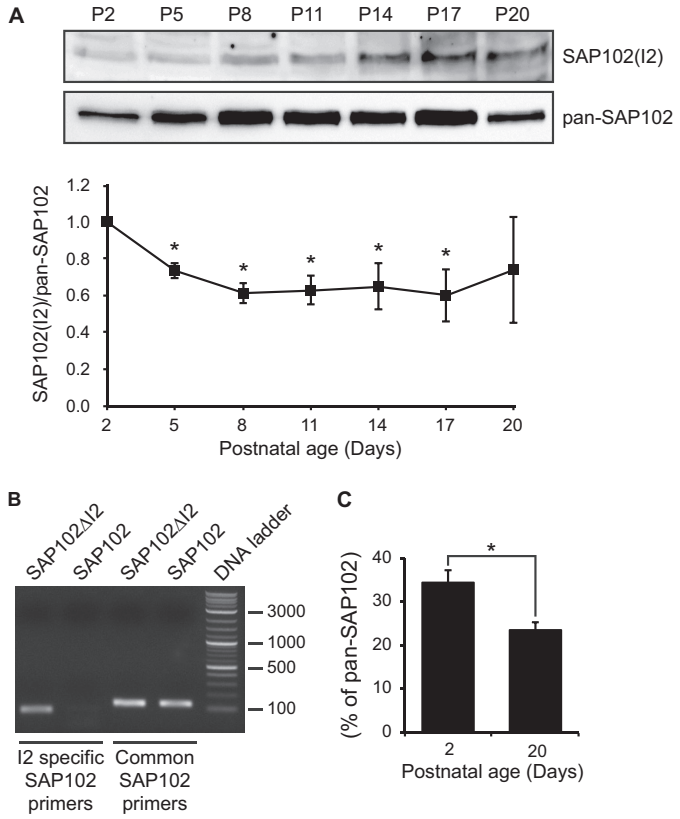

FIGURE 4. **SAP102 splice variants are developmentally regulated.** *A*, whole rat brain lysate was collected at various ages. The P2 fraction was isolated and resolved by 10% SDS-PAGE. Samples were immunoblotted with either pan-SAP102 antibody or with I2-specific SAP102 antibody. The experiment was repeated three times and quantified using ImageQuant LAS TL software. A representative blot is shown in *A*. All ages were normalized to the intensity at P2, and a ratio of SAP102(I2) to total SAP102 was determined. Data represent the means ± S.E. (*, $p < 0.05$, one-sample *t* test). *B*, specificity of I2-specific and common SAP102 primers was confirmed by PCR with FLAG-SAP102ΔI2 and FLAG-SAP102. *C*, the mRNA levels of SAP102(I2) were measured by performing real-time PCR with cDNA from mouse cortex at postnatal day 2 and 20. Samples were run in triplicate ($n = 3$). Data represent the means ± S.E. (*, $p < 0.05$, Student's *t* test).

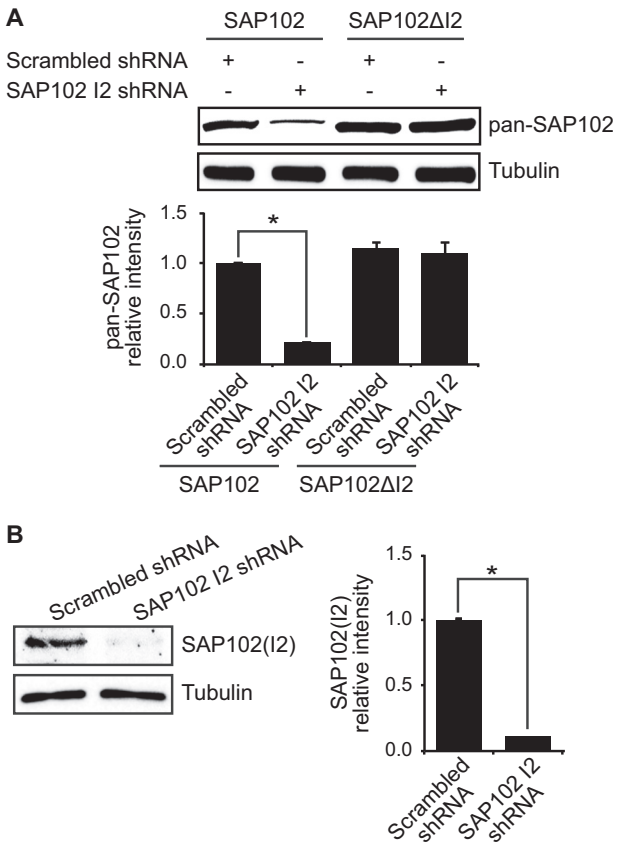

FIGURE 5. **shRNA knockdown of endogenous I2-containing SAP102.** *A*, HEK-293 cells were co-transfected with SAP102 or SAP102ΔI2 and scrambled shRNA or SAP102 I2 shRNA, and the immunoblots of cell lysate were probed with pan-SAP102 or tubulin antibody. Data represent the means ± S.E. ($n = 3$ independent experiments; *, $p < 0.05$, Student's *t* test). *B*, primary cortical neurons (DIV4) were infected with lentivirus containing SAP102 I2 shRNA or scrambled shRNA. The cell lysates were prepared at DIV14, resolved by SDS-PAGE, and immunoblotted with I2-specific SAP102 or tubulin antibody. Data represent the means ± S.E. ($n = 3$ independent experiments; *, $p < 0.05$, Student's *t* test).

NMDAR surface expression (Fig. 6, *A* and *B*). To determine whether surface expression of endogenous GluN2A and GluN2B is regulated by I2 region-containing SAP102, we infected cultured cortical neurons with lentivirus expressing SAP102 I2 shRNA at DIV4 and performed a cell surface biotinylation assay at DIV14. We biotinylated neurons for 20 min at 4 °C, isolated surface-expressed proteins with NeutrAvidin beads, and probed immunoblots with antibodies to detect surface-expressed pools of receptor. Tubulin, a cytosolic protein, was used as a negative control for surface biotinylation, confirming the specificity of our biotinylation procedure (Fig. 6*C*). Using this independent biochemical assay, we found that surface expression of GluN2A increased substantially upon knocking down the I2 region-containing SAP102 (Fig. 6, *C* and *D*). However, we observed no change in GluN2B surface expression (Fig. 6, *C* and *D*). We next tested whether subunit-specific regulation of NMDAR surface expression by SAP102 is isoform-specific. Cultured cortical neurons were infected with lentivirus expressing a previously characterized SAP102 I1 shRNA that selectively knocked down expression of I1 region-containing SAP102 (16). In previous studies we have shown that I1 region-containing SAP102 mediates synaptic removal of GluN2B-containing NMDARs (15). Consistently, we found that surface expression of GluN2B was substantially increased upon knocking down the I1 region-containing SAP102, whereas surface expression of GluN2A was not changed (Fig. 6, *E* and *F*). These findings corroborate with our imaging data, indicating that SAP102 plays an important role in the regulation of the subunit composition of surface NMDARs.

DISCUSSION

In this study we provide evidence for a novel mechanism for the subunit-specific regulation of NMDARs. First, we show that synaptic targeting of SAP102 is regulated by C-terminal splicing. The SAP102 splice variant containing the I2 region is preferentially targeted to dendritic spines compared with splice variant with this region deleted. Second, we show that there is an intramolecular interaction between the SH3 and GK domains in SAP102 but that the SH3-GK interaction is not affected by removal of the I2 region. Third, we find that spine lengthening induced by SAP102 expression is not dependent on the I2 region. Fourth, we show that expression of SAP102(I2) is developmentally regulated with a higher proportion of the I2

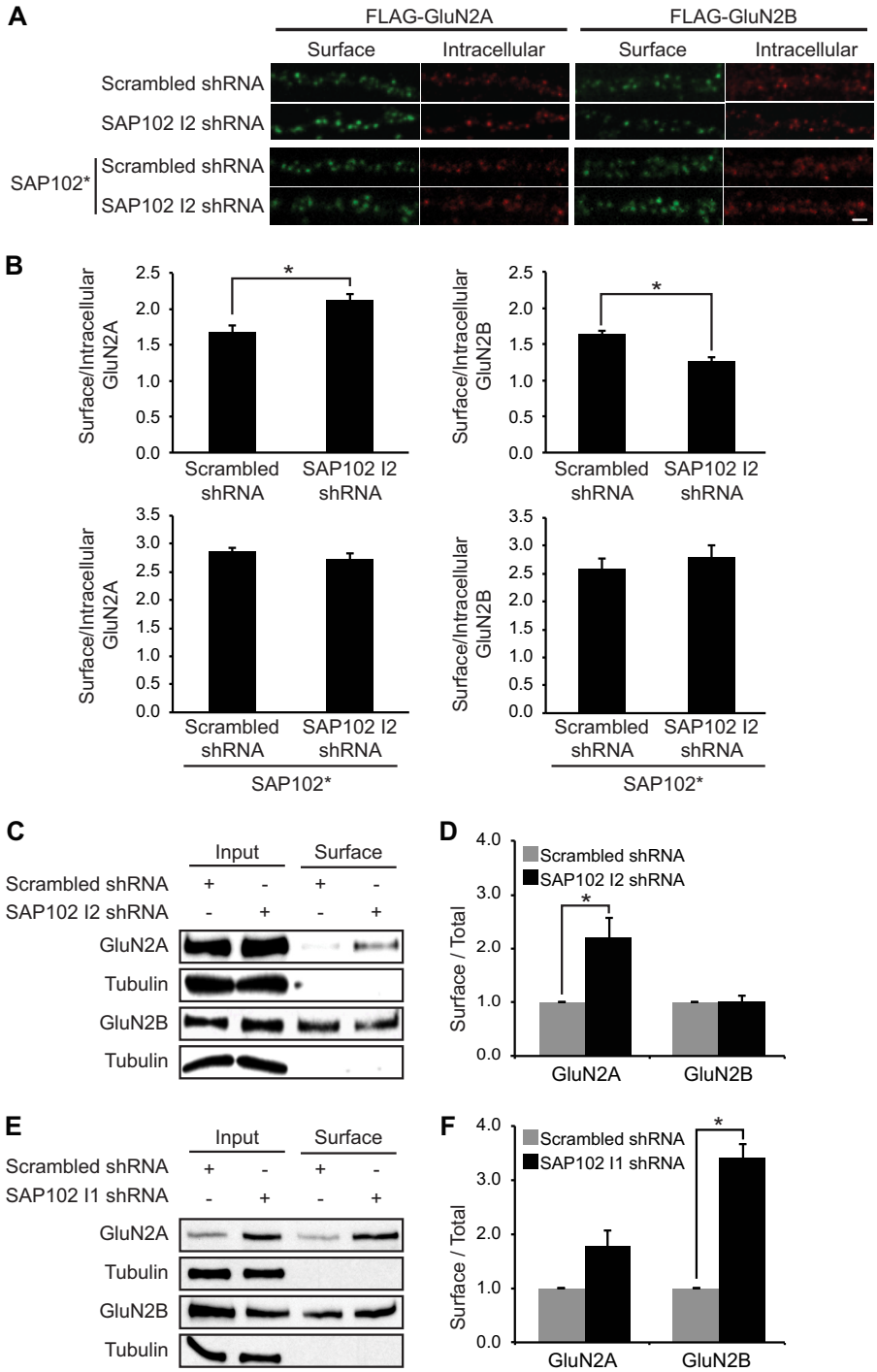

FIGURE 6. **Knock-down of I2-containing SAP102 increases surface expression of GluN2A.** *A*, I2-containing SAP102 was knocked down in hippocampal cultures by the lentiviral induction of SAP102 I2 shRNA at DIV4, and FLAG-tagged GluN2A or GluN2B was transfected at DIV12. *B*, co-transfection of FLAG-tagged GluN2A or GluN2B with an shRNA-proofed Myc-tagged SAP102 variant (*SAP102**). Surface staining was performed at DIV14 with anti-FLAG and Alexa 647 secondary antibodies (*green*), and after permeabilization, the intracellular pool was labeled with anti-FLAG and Alexa 568 secondary antibodies (*red*). *Scale bar*, 2 μm. *B*, quantification of the imaging experiments. Fluorescence intensities were measured using ImageJ software. Data represent the means ± S.E. ($n = 27$; $n = 3$ independent experiments); *, $p < 0.05$, Student's *t* test. *C*, biotinylated surface proteins from cortical neurons infected with lentivirus containing scrambled or SAP102 I2 shRNA were isolated, resolved by SDS-PAGE, and probed with GluN2A, GluN2B, or α-tubulin antibodies. *D*, quantification of the biotinylation experiments. The immunoreactive signals for surface GluN2A and GluN2B were normalized to total input and presented as a *bar graph*. $n = 3$ independent experiments. Data represent the mean ± S.E.; *, $p < 0.05$, Student's *t* test. *E*, biotinylated surface proteins from cortical neurons infected with lentivirus containing scrambled or SAP102 I1 shRNA were isolated, resolved by SDS-PAGE, and probed with GluN2A, GluN2B, or α-tubulin antibodies. *F*, quantification of the biotinylation experiments. The immune-reactive signals for surface GluN2A and GluN2B were normalized to total input and presented as a *bar graph*. $n = 3$ independent experiments. Data represent the means ± S.E.; *, $p < 0.05$, Student's *t* test.

region-containing SAP102 isoforms during early development. Finally, we show that knocking down SAP102(I2) increases surface expression of GluN2A. Thus, our findings suggest an important role of SAP102 synaptic targeting in modulating the GluN2 subunit composition of NMDARs at synapses.

PSD-MAGUKs are involved in the anchoring of various transmembrane proteins including NMDARs and AMPA receptors (1). In addition, they act as scaffolds to bring signaling complexes together and to link receptors to downstream signaling cascades. PSD-MAGUKs are highly enriched at the PSD. Studies have shown that synaptic localization of PSD-95 is regulated by post-translational modifications (21–23). For example, PSD-95 contains two cysteine residues in the N terminus that can be palmitoylated (31). Palmitoylation of PSD-95 is required for its postsynaptic targeting and subsequent ion channel clustering (22). Moreover, PSD-95 palmitoylation can be dynamically modulated by synaptic activity (32). In contrast, SAP102 is not palmitoylated, and how SAP102 is targeted to synapses is not clear. Using protein domain truncation approaches, it has been shown that synaptic localization of SAP102 is dependent on the SH3 and GK domains (19). The different mechanisms by which PSD-95 and SAP102 are targeted to synapses suggest that they play distinct roles in receptor stabilization and/or trafficking at synapses. Indeed, SAP102 is highly mobile in dendritic spines compared with PSD-95 and has recently been shown to mediate synaptic removal of GluN2B-containing NMDARs (15). We have now identified an alternatively spliced region I2 between the SH3 and GK domains that is important for SAP102 synaptic targeting, indicating that synaptic localization of SAP102 is regulated by splicing events.

Previous studies have shown that synaptic targeting of SAP97 is dependent on the presence of a specific alternatively spliced insertion called the I3 region (33). Similar to the I2 region of SAP102, the I3 region of SAP97 is also localized within the hinge region between the SH3 and GK domains. It has been shown that the I3 region of the human homologue of SAP97 interacts with an actin/spectrin-binding protein, protein 4.1, and both proteins colocalize to membranes and regions of cell-cell contact in human MCF-7 cells (34). Subsequent studies using cultured rat neurons have found that SAP97 association with protein 4.1 is critical for targeting SAP97 to dendritic spines (33). Interestingly, recent studies have shown that SAP97 containing the I3 region specifically binds to Ca^{2+}/calmodulin-dependent protein kinase II (CaMKII), and CaMKII phosphorylation of SAP97 disrupts its interaction with protein kinase A anchoring protein 79/150 (AKAP79/150) (35). Whether CaMKII binding to SAP97 regulates its interaction with protein 4.1 and synaptic targeting is not known. Upon sequence examination, we did not find any significant similarity between the I3 region (34 aa) of SAP97 and the I2 region (14 aa) of SAP102. Therefore, it is unlikely that protein 4.1 plays a role in synaptic targeting of I2-containing SAP102 isoforms. However, it will be of interest for future studies to determine whether the I2 region of SAP102 contains protein-protein interacting motif.

The crystal structure of the SH3-GK module from PSD-95 has been solved (36, 37). It supports the yeast two-hybrid intramolecular interaction data showing that the SH3-GK module can assemble in either an intra- or intermolecular fashion. Interestingly, the hinge region linking the two interacting domains plays a key role in determining the preference for intra- *versus* intermolecular assembly (36). Although the SH3 and GK domains of SAP102 are highly homologous to those of PSD-95, the intramolecular interaction between the SH3 and GK domains in SAP102 has never been tested. Therefore, we used the yeast two-hybrid assay and found that indeed there is an intramolecular interaction between the SH3 and GK domains in SAP102. We also examined the effect of the I2 region on intramolecular interaction and observed no change in binding when I2 was deleted, suggesting that the I2 region in not involved in the intramolecular interaction. However, it has been proposed that protein binding to the hinge region may constrain this region to promote intermolecular assembly at specific membrane sites (36). Thus, instead of directly modulating the intramolecular interaction, the I2 region may contain a regulatory protein binding site, thereby promoting a switch from intra- to intermolecular assembly upon protein binding.

Accumulating evidence has indicated that morphological changes of dendritic spines represent a key mechanism underlying plasticity of brain function. Studies have shown that synaptic properties including number and type of receptors, calcium dynamics, and synaptic plasticity are linked to changes in dendritic spine morphology. For example, growth and/or enlargement of spines are associated with induction of long term potentiation, whereas induction of long term depression causes shrinkage and/or retraction of spines (38–41). Early in development, dendrites have longer, thinner filopodia that facilitate synaptogenesis by initiating axonal contact, which subsequently leads to synapse formation (42). We and others have shown that neurons expressing SAP102 have significantly longer dendritic spines, implying a role for SAP102 in synaptogenesis (16, 28). We further demonstrate that the spine lengthening effect of SAP102 is dependent on the presence of specific alternatively spliced region I1 in the N terminus as well as NMDAR activity (16). Here, we show that spine length also increases in neurons expressing SAP102ΔI2, indicating that the I2 region is not required for SAP102-dependent spine lengthening. In addition, neurons expressing SAP102ΔSH3GK exhibit similar spine length as SAP102 expressing neurons. Although SAP102ΔSH3GK is not enriched in dendritic spines, which is different from SAP102 and SAP102ΔI2, it contains the I1 region and is localized at spines, indicating that the I1 region of SAP102 is critical for the spine lengthening effect.

SAP102 is the dominant PSD-MAGUK protein during early postnatal development. Although SAP102 deletion causes embryonic lethality with low penetrance (43), SAP102 null mice that survive into adulthood show impairments in synaptic plasticity and spatial learning (3). Accordingly, recent studies have demonstrated that SAP102 plays an important role in excitatory synapse formation (44). These findings are consistent with earlier electrophysiological studies showing that SAP102 regulates glutamate receptor trafficking during synaptogenesis (8). Interestingly, mutations in the human gene encoding SAP102 are associated with X-linked intellectual dis-

ability, which is often associated with dendritic spine abnormalities (45–47). Protein products of all identified SAP102 mutant alleles lack the SH3 and GK domains, which could lead to mislocalization of the truncated SAP102 protein and disruption of the downstream signaling of NMDARs.

During development, synaptic NMDAR subunit composition changes from primarily GluN2B- to GluN2A-containing receptors. Because GluN2A- and GluN2B-containing NMDARs exhibit different channel kinetics and open probabilities (48), this developmental switch results in changes in the functional properties of synaptic NMDARs. Studies have shown that the subunit switch is activity- and experience-dependent and can be controlled by certain forms of synaptic plasticity (49–53). For example, long-term potentiation induction causes a rapid switch in GluN2 subunit composition of synaptic NMDARs at neonatal synapses (50). The subunit switch induced by long-term potentiation requires activation of NMDARs and mGluR5 (54). However, the molecular mechanisms that account for the subunit switch remain unclear. It is generally believed that PSD-MAGUKs play an important role in the GluN2 subunit switch during development. Studies have shown that PSD-95 overexpression in cultured cerebellar granule cells promotes synaptic expression of GluN2A-containing receptors (55). Additionally, eye opening induces a rapid dendritic localization of PSD-95, which is bound to more GluN2A-containing NMDARs (56). Another line of evidence comes from the studies using PSD-95 knock out mice or PSD-95/PSD-93 double knock-out mice showing that the contribution of GluN2B-containing receptors to the NMDAR-mediated synaptic current is greater compared with wild-type animals (8, 57). It is clear that PSD-95 regulates the GluN2 subunit switch. Whether other PSD-MAGUKs play a role in the regulation of NMDAR subunit composition is not known.

We now provide evidence that SAP102 is involved in modulating the subunit composition of surface NMDARs. Using a combination of imaging and biochemical approaches, we demonstrated a specific enhancement of GluN2A surface expression upon knocking down I2-containing SAP102. Although a concurrent decrease of GluN2B on the surface of hippocampal neurons was observed in our imaging data, the surface biotinylation assays did not show any significant change in GluN2B surface expression upon SAP102(I2) knockdown in cultured cortical neurons. This discrepancy may result from different experimental conditions between these two approaches. The surface biotinylation assays exam the surface expression of endogenous GluN2A and GluN2B, whereas the imaging experiments measure surface expression of exogenously expressed receptors. Nevertheless, our data have conclusively shown that I2-containing SAP102 regulates NMDAR subunit composition. The specific increase in GluN2A surface expression inevitably modifies the GluN2A/GluN2B ratio, which has been shown to be critical in regulating the threshold for bidirectional synaptic plasticity (11). In addition, the timing of decreased expression of I2-containing SAP102 correlates well with the GluN2 subunit switch during development. Together, our findings suggest that synaptic enrichment of SAP102 plays an important role in regulating subunit composition of NMDARs at synapses. Whether SAP102 directly regulates GluN2A trafficking or increase of GluN2A surface expression results from synaptic replacement of SAP102 by PSD-95 is unclear and will be of interest to study in future work.

Acknowledgments—We thank Katherine Roche for critical reading of the manuscript and Jimok Kim for helpful discussions.

REFERENCES

1. Elias, G. M., and Nicoll, R. A. (2007) Synaptic trafficking of glutamate receptors by MAGUK scaffolding proteins. *Trends Cell Biol.* **17,** 343–352
2. El-Husseini, A. E., Topinka, J. R., Lehrer-Graiwer, J. E., Firestein, B. L., Craven, S. E., Aoki, C., and Bredt, D. S. (2000) Ion channel clustering by membrane-associated guanylate kinases. Differential regulation by N-terminal lipid and metal binding motifs. *J. Biol. Chem.* **275,** 23904–23910
3. Cuthbert, P. C., Stanford, L. E., Coba, M. P., Ainge, J. A., Fink, A. E., Opazo, P., Delgado, J. Y., Komiyama, N. H., O'Dell, T. J., and Grant, S. G. (2007) Synapse-associated protein 102/dlgh3 couples the NMDA receptor to specific plasticity pathways and learning strategies. *J. Neurosci.* **27,** 2673–2682
4. Sans, N., Petralia, R. S., Wang, Y. X., Blahos, J., 2nd, Hell, J. W., and Wenthold, R. J. (2000) A developmental change in NMDA receptor-associated proteins at hippocampal synapses. *J. Neurosci.* **20,** 1260–1271
5. Sans, N., Prybylowski, K., Petralia, R. S., Chang, K., Wang, Y. X., Racca, C., Vicini, S., and Wenthold, R. J. (2003) NMDA receptor trafficking through an interaction between PDZ proteins and the exocyst complex. *Nat. Cell Biol.* **5,** 520–530
6. Washbourne, P., Liu, X. B., Jones, E. G., and McAllister, A. K. (2004) Cycling of NMDA receptors during trafficking in neurons before synapse formation. *J. Neurosci.* **24,** 8253–8264
7. El-Husseini, A. E., Schnell, E., Chetkovich, D. M., Nicoll, R. A., and Bredt, D. S. (2000) PSD-95 involvement in maturation of excitatory synapses. *Science* **290,** 1364–1368
8. Elias, G. M., Elias, L. A., Apostolides, P. F., Kriegstein, A. R., and Nicoll, R. A. (2008) Differential trafficking of AMPA and NMDA receptors by SAP102 and PSD-95 underlies synapse development. *Proc. Natl. Acad. Sci. U.S.A.* **105,** 20953–20958
9. Cull-Candy, S. G., and Leszkiewicz, D. N. (2004) Role of distinct NMDA receptor subtypes at central synapses. *Sci. STKE 2004,* re16
10. Traynelis, S. F., Wollmuth, L. P., McBain, C. J., Menniti, F. S., Vance, K. M., Ogden, K. K., Hansen, K. B., Yuan, H., Myers, S. J., and Dingledine, R. (2010) Glutamate receptor ion channels: structure, regulation, and function. *Pharmacol. Rev.* **62,** 405–496
11. Yashiro, K., and Philpot, B. D. (2008) Regulation of NMDA receptor subunit expression and its implications for LTD, LTP, and metaplasticity. *Neuropharmacology* **55,** 1081–1094
12. Barria, A., and Malinow, R. (2005) NMDA receptor subunit composition controls synaptic plasticity by regulating binding to CaMKII. *Neuron* **48,** 289–301
13. van Zundert, B., Yoshii, A., and Constantine-Paton, M. (2004) Receptor compartmentalization and trafficking at glutamate synapses: a developmental proposal. *Trends Neurosci.* **27,** 428–437
14. Müller, B. M., Kistner, U., Kindler, S., Chung, W. J., Kuhlendahl, S., Fenster, S. D., Lau, L. F., Veh, R. W., Huganir, R. L., Gundelfinger, E. D., and Garner, C. C. (1996) SAP102, a novel postsynaptic protein that interacts with NMDA receptor complexes *in vivo*. *Neuron* **17,** 255–265
15. Chen, B. S., Gray, J. A., Sanz-Clemente, A., Wei, Z., Thomas, E. V., Nicoll, R. A., and Roche, K. W. (2012) SAP102 mediates synaptic clearance of NMDA receptors. *Cell Reports* **2,** 1120–1128
16. Chen, B. S., Thomas, E. V., Sanz-Clemente, A., and Roche, K. W. (2011) NMDA receptor-dependent regulation of dendritic spine morphology by SAP102 splice variants. *J. Neurosci.* **31,** 89–96

17. Chen, B. S., and Roche, K. W. (2009) Growth factor-dependent trafficking of cerebellar NMDA receptors via protein kinase B/Akt phosphorylation of NR2C. *Neuron* **62,** 471–478
18. Chen, B. S., Braud, S., Badger, J. D., 2nd, Isaac, J. T., and Roche, K. W. (2006) Regulation of NR1/NR2C *N*-methyl-D-aspartate (NMDA) receptors by phosphorylation. *J. Biol. Chem.* **281,** 16583–16590
19. Zheng, C. Y., Petralia, R. S., Wang, Y. X., Kachar, B., and Wenthold, R. J. (2010) SAP102 is a highly mobile MAGUK in spines. *J. Neurosci.* **30,** 4757–4766
20. Xu, W. (2011) PSD-95-like membrane associated guanylate kinases (PSD-MAGUKs) and synaptic plasticity. *Curr. Opin. Neurobiol.* **21,** 306–312
21. Kim, M. J., Futai, K., Jo, J., Hayashi, Y., Cho, K., and Sheng, M. (2007) Synaptic accumulation of PSD-95 and synaptic function regulated by phosphorylation of serine 295 of PSD-95. *Neuron* **56,** 488–502
22. El-Husseini, A. E., Craven, S. E., Chetkovich, D. M., Firestein, B. L., Schnell, E., Aoki, C., and Bredt, D. S. (2000) Dual palmitoylation of PSD-95 mediates its vesiculotubular sorting, postsynaptic targeting, and ion channel clustering. *J. Cell Biol.* **148,** 159–172
23. Colledge, M., Snyder, E. M., Crozier, R. A., Soderling, J. A., Jin, Y., Langeberg, L. K., Lu, H., Bear, M. F., and Scott, J. D. (2003) Ubiquitination regulates PSD-95 degradation and AMPA receptor surface expression. *Neuron* **40,** 595–607
24. Goebel-Goody, S. M., Davies, K. D., Alvestad Linger, R. M., Freund, R. K., and Browning, M. D. (2009) Phospho-regulation of synaptic and extrasynaptic *N*-methyl-D-aspartate receptors in adult hippocampal slices. *Neuroscience* **158,** 1446–1459
25. Shin, H., Hsueh, Y. P., Yang, F. C., Kim, E., and Sheng, M. (2000) An intramolecular interaction between Src homology 3 domain and guanylate kinase-like domain required for channel clustering by postsynaptic density-95/SAP90. *J. Neurosci.* **20,** 3580–3587
26. McGee, A. W., and Bredt, D. S. (1999) Identification of an intramolecular interaction between the SH3 and guanylate kinase domains of PSD-95. *J. Biol. Chem.* **274,** 17431–17436
27. Wu, H., Reissner, C., Kuhlendahl, S., Coblentz, B., Reuver, S., Kindler, S., Gundelfinger, E. D., and Garner, C. C. (2000) Intramolecular interactions regulate SAP97 binding to GKAP. *EMBO J.* **19,** 5740–5751
28. Sans, N., Wang, P. Y., Du, Q., Petralia, R. S., Wang, Y. X., Nakka, S., Blumer, J. B., Macara, I. G., and Wenthold, R. J. (2005) mPins modulates PSD-95 and SAP102 trafficking and influences NMDA receptor surface expression. *Nat. Cell Biol.* **7,** 1179–1190
29. Kim, E., Naisbitt, S., Hsueh, Y. P., Rao, A., Rothschild, A., Craig, A. M., and Sheng, M. (1997) GKAP, a novel synaptic protein that interacts with the guanylate kinase-like domain of the PSD-95/SAP90 family of channel clustering molecules. *J. Cell Biol.* **136,** 669–678
30. Pak, D. T., Yang, S., Rudolph-Correia, S., Kim, E., and Sheng, M. (2001) Regulation of dendritic spine morphology by SPAR, a PSD-95-associated RapGAP. *Neuron* **31,** 289–303
31. Topinka, J. R., and Bredt, D. S. (1998) N-terminal palmitoylation of PSD-95 regulates association with cell membranes and interaction with K^+ channel Kv1.4. *Neuron* **20,** 125–134
32. El-Husseini Ael-D., Schnell, E., Dakoji, S., Sweeney, N., Zhou, Q., Prange, O., Gauthier-Campbell, C., Aguilera-Moreno, A., Nicoll, R. A., and Bredt, D. S. (2002) Synaptic strength regulated by palmitate cycling on PSD-95. *Cell* **108,** 849–863
33. Rumbaugh, G., Sia, G. M., Garner, C. C., and Huganir, R. L. (2003) Synapse-associated protein-97 isoform-specific regulation of surface AMPA receptors and synaptic function in cultured neurons. *J. Neurosci.* **23,** 4567–4576
34. Lue, R. A., Marfatia, S. M., Branton, D., and Chishti, A. H. (1994) Cloning and characterization of hdlg: the human homologue of the *Drosophila* discs large tumor suppressor binds to protein 4.1. *Proc. Natl. Acad. Sci. U.S.A.* **91,** 9818–9822
35. Nikandrova, Y. A., Jiao, Y., Baucum, A. J., Tavalin, S. J., and Colbran, R. J. (2010) Ca^{2+}/calmodulin-dependent protein kinase II binds to and phosphorylates a specific SAP97 splice variant to disrupt association with AKAP79/150 and modulate α-amino-3-hydroxy-5-methyl-4-isoxazolepropionic acid-type glutamate receptor (AMPAR) activity. *J. Biol. Chem.* **285,** 923–934
36. McGee, A. W., Dakoji, S. R., Olsen, O., Bredt, D. S., Lim, W. A., and Prehoda, K. E. (2001) Structure of the SH3-guanylate kinase module from PSD-95 suggests a mechanism for regulated assembly of MAGUK scaffolding proteins. *Mol. Cell* **8,** 1291–1301
37. Tavares, G. A., Panepucci, E. H., and Brunger, A. T. (2001) Structural characterization of the intramolecular interaction between the SH3 and guanylate kinase domains of PSD-95. *Mol. Cell* **8,** 1313–1325
38. Matsuzaki, M., Honkura, N., Ellis-Davies, G. C., and Kasai, H. (2004) Structural basis of long-term potentiation in single dendritic spines. *Nature* **429,** 761–766
39. Nägerl, U. V., Eberhorn, N., Cambridge, S. B., and Bonhoeffer, T. (2004) Bidirectional activity-dependent morphological plasticity in hippocampal neurons. *Neuron* **44,** 759–767
40. Okamoto, K., Nagai, T., Miyawaki, A., and Hayashi, Y. (2004) Rapid and persistent modulation of actin dynamics regulates postsynaptic reorganization underlying bidirectional plasticity. *Nat. Neurosci.* **7,** 1104–1112
41. Zhou, Q., Homma, K. J., and Poo, M. M. (2004) Shrinkage of dendritic spines associated with long-term depression of hippocampal synapses. *Neuron* **44,** 749–757
42. Yoshihara, Y., De Roo, M., and Muller, D. (2009) Dendritic spine formation and stabilization. *Curr. Opin. Neurobiol.* **19,** 146–153
43. Van Campenhout, C. A., Eitelhuber, A., Gloeckner, C. J., Giallonardo, P., Gegg, M., Oller, H., Grant, S. G., Krappmann, D., Ueffing, M., and Lickert, H. (2011) Dlg3 trafficking and apical tight junction formation is regulated by nedd4 and nedd4–2 e3 ubiquitin ligases. *Dev. Cell* **21,** 479–491
44. Murata, Y., and Constantine-Paton, M. (2013) Postsynaptic density scaffold SAP102 regulates cortical synapse development through EphB and PAK signaling pathway. *J. Neurosci.* **33,** 5040–5052
45. Tarpey, P., Parnau, J., Blow, M., Woffendin, H., Bignell, G., Cox, C., Cox, J., Davies, H., Edkins, S., Holden, S., Korny, A., Mallya, U., Moon, J., O'Meara, S., Parker, A., Stephens, P., Stevens, C., Teague, J., Donnelly, A., Mangelsdorf, M., Mulley, J., Partington, M., Turner, G., Stevenson, R., Schwartz, C., Young, I., Easton, D., Bobrow, M., Futreal, P. A., Stratton, M. R., Gecz, J., Wooster, R., and Raymond, F. L. (2004) Mutations in the DLG3 gene cause nonsyndromic X-linked mental retardation. *Am. J. Hum. Genet.* **75,** 318–324
46. Zanni, G., van Esch, H., Bensalem, A., Saillour, Y., Poirier, K., Castelnau, L., Ropers, H. H., de Brouwer, A. P., Laumonnier, F., Fryns, J. P., and Chelly, J. (2010) A novel mutation in the DLG3 gene encoding the synapse-associated protein 102 (SAP102) causes non-syndromic mental retardation. *Neurogenetics* **11,** 251–255
47. Philips, A. K., Sirén, A., Avela, K., Somer, M., Peippo, M., Ahvenainen, M., Doagu, F., Arvio, M., Kääriäinen, H., Van Esch, H., Froyen, G., Haas, S. A., Hu, H., Kalscheuer, V. M., and Järvelä, I. (2014) X-exome sequencing in Finnish families with Intellectual Disability - four novel mutations and two novel syndromic phenotypes. *Orphanet. J. Rare Dis.* **9,** 49
48. Paoletti, P., Bellone, C., and Zhou, Q. (2013) NMDA receptor subunit diversity: impact on receptor properties, synaptic plasticity and disease. *Nat. Rev. Neurosci.* **14,** 383–400
49. Barria, A., and Malinow, R. (2002) Subunit-specific NMDA receptor trafficking to synapses. *Neuron* **35,** 345–353
50. Bellone, C., and Nicoll, R. A. (2007) Rapid bidirectional switching of synaptic NMDA receptors. *Neuron* **55,** 779–785
51. Gray, J. A., Shi, Y., Usui, H., During, M. J., Sakimura, K., and Nicoll, R. A. (2011) Distinct modes of AMPA receptor suppression at developing synapses by GluN2A and GluN2B: single-cell NMDA receptor subunit deletion in vivo. *Neuron* **71,** 1085–1101
52. Sanz-Clemente, A., Matta, J. A., Isaac, J. T., and Roche, K. W. (2010) Casein kinase 2 regulates the NR2 subunit composition of synaptic NMDA receptors. *Neuron* **67,** 984–996
53. Philpot, B. D., Sekhar, A. K., Shouval, H. Z., and Bear, M. F. (2001) Visual experience and deprivation bidirectionally modify the composition and function of NMDA receptors in visual cortex. *Neuron* **29,** 157–169
54. Matta, J. A., Ashby, M. C., Sanz-Clemente, A., Roche, K. W., and Isaac, J. T.

(2011) mGluR5 and NMDA receptors drive the experience- and activity-dependent NMDA receptor NR2B to NR2A subunit switch. *Neuron* **70,** 339–351

55. Losi, G., Prybylowski, K., Fu, Z., Luo, J., Wenthold, R. J., and Vicini, S. (2003) PSD-95 regulates NMDA receptors in developing cerebellar granule neurons of the rat. *J. Physiol.* **548,** 21–29
56. Yoshii, A., Sheng, M. H., and Constantine-Paton, M. (2003) Eye opening induces a rapid dendritic localization of PSD-95 in central visual neurons. *Proc. Natl. Acad. Sci. U.S.A.* **100,** 1334–1339
57. Béïque, J. C., Lin, D. T., Kang, M. G., Aizawa, H., Takamiya, K., and Huganir, R. L. (2006) Synapse-specific regulation of AMPA receptor function by PSD-95. *Proc. Natl. Acad. Sci. U.S.A.* **103,** 19535–19540